Acta Scientific Pharmaceutical Sciences

Volume 1 Issue 3 September 2017

Research Article

Identifying and Predicting the Effectiveness of Fenretinide (4-HPR) Alone or in Combination with Radiotherapy

Emad Y Moawad[1,2]*

[1]*Researcher graduated from Ain Shams University, Cairo, Egypt Department of Engineering, Cairo, Egypt*

[2]*A member of the Korean Society of Nuclear Medicine and of the World Conference of Interventional Oncology (WCIO) USA*

***Corresponding Author:** Emad Y Moawad, Researcher graduated from Ain Shams University, Cairo, Egypt Department of Engineering, Alhegaz Street, Alnozha, Cairo, Egypt.

Received: June 08, 2017; **Published:** August 22, 2017

Abstract

Optimizing Fenretinide (4-HPR) therapy requires predicting patient's response to the personalized dose before therapy. This research aims to identify and predict the effectiveness of 4-HPR alone or in combination with radiotherapy. Models involving *in-vivo* i.p. growth of non-small cell lung cancer (NSCLC), Ramos Burkitt lymphoma and pediatric tumor alveolar rhabdomyosarcoma (aRMS) in athymic nude mice were used. Nine doses of (10 mg/kg, 40 mg/kg) or (single dose of 30 mg/kg or 10 Gy radiotherapy alone or in combination), 20 doses of 12.5 mg/kg and 14 doses of 20mg/kg of 4-HPR in those xenograft growths were respectively applied. *In-vitro* -Thymidine proliferation assay was also performed on samples of Ramos AW cell line incubated with 0.1, 1 and 10 M of 4-HPR. A prediction to the response of cancer to 4-HPR was conducted as described before in earlier studies. Energy of the influence following therapy was perfectly correlated (r = 1) with 4-HPR dose. An efficient dose-energy model was established with a perfect fit (R^2= 1) estimates the energy yield by 4-HPR dose. The response of each of Ramos AW cell line and aRMS model to 4-HPR alone and NSCLC model to 4-HPR alone or in combination with radiotherapy were predicted 100% identical to the actual *in-vitro* and *in-vivo* responses. Efficacy of 4-HPR is identical in both assays regardless to stage or type of disease and predictable whether applied alone or in combination with radiotherapy. Targeting patient-personalized medicine, dose-energy model of 4-HPR is reliable to predict patient's response before therapy to avoid chemo-resistance and treatment failure.

Keywords: Non-Small Cell Lung Cancer; Ramos Burkitt Lymphoma and Pediatric Tumor Alveolar Rhabdomyosarcoma; Ramos AW Cell Line; Fenretinide; Dose-Energy Model; Radiotherapy

Introduction

Retinoids are a class of drugs constitutes a family of vitamin A derivatives regulate epithelial cell proliferation, cell differentiation, apoptosis during embryonic development and in maintaining the differentiated status of adult tissues [1]. Retinoids have several important and diverse functions in immune system activate tumor suppressor genes to be considered a promising class of anti-cancer agents for the treatment, prevention of a number of malignancies and some second cancers [2]. Clinical trials have shown that retinoids are active in treatment of heterogeneous type of tumors, like breast cancer in which effective responses of breast tumor cells to all trans- retinoic acid (ATRA), the prototype of retinoids were confirmed [3]. The synthetic retinoid N-(4-hydroxyphenyl) retinamide (4-HPR, fenretinide) has potential as a promising chemotherapeutic drug due to its strong pro-apoptotic effect on a variety of tumors especially on lung cancer [4], prostate cancer [5], bladder cancer [6], acute lymphoblastic leukemia (ALL) cell lines [7,8], and on neuroblastoma besides to breast cancer [9]. 4- HPR is currently being applied in several clinical trials against different tumors [10,11] and has been shown to overcome tumor resistance to ATRA [12]. Although the ability of 4-HPR to inhibit growth of cancer and metastasis has been confirmed *in vitro* and *in vivo*, no relationship has been determined between such ability in each assay. These different measures in both assays should be linked together such that from the in-vivo measurements, the *in-vitro* ones can be predicted and vice versa. Prediction of the *in-vivo* and *in-vitro* responses to 4-HPR prior to therapy aims to administer the personalized dose that contributes to optimize therapy and consequently decrease the risks of chemo-resistance or treatment failure. On the other hand, earlier studies have shown that the addition of concurrent retinoids to radiotherapy enhances the ability of radiation to kill cells and induce apoptosis in a wide variety of tumors including lung cancer cells [13-15]. Thus far, however, no study has evaluated precisely the antitumor effect of 4-HPR alone or in combination with radiotherapy so that differentiating between these therapies will be based on predicting their outcomes. Moawad has introduced clinical and pathological staging models in which grade of the disease can be identified [16-23]. Those staging models have

been used also to construct dose-energy models of some antineoplastic drugs through either of the *in-vitro* or the *in-vivo* responses to those drugs [24-32]. Hereby, in this research those staging models were applied to identify and predict the effectiveness of 4-HPR *in-vitro* and *in-vivo* alone or in combination with radiotherapy.

Materials and Methods

Model of Identifying Effectiveness of Drug Dose *in-vitro*

Targeting patient-personalized medicine, Moawad presented recently a model for evaluating effectiveness of therapy at the cellular level by identifying patient-specific histologic grade (H_G) before and after therapy [24-32]. In such model, Cell Growth Energy (CGE) expresses rate of cell proliferation, where

$$CGE = \ln\left[\ln\frac{\ln 2}{t_D}\right]^2 Emad \quad \text{(Equation 1)},$$

Emad = 23234.59 MeV (Equation 2) and t_D is the cell doubling time. While H_G is the summation of CGE of the biological culture (sample). i.e. $H_G = \sum CGE \times 23234.59$ MeV (Equation 3) [16-32]. On the other hand, H_G in case of constancy in number of cells can be identified *in vitro* through Tritiated Thymidine (^{3}H -TDR) proliferation assay as follows: $H_G = U\% \times E_{3_{H\text{-}TDR}}$ MeV (Equation 4), where U% is the unlabeled fraction of the detected sample of cells by ^{3}H-TDR [U%=1-Labelled index (Li)] and $E_{3_{H\text{-}TDR}}$ is the energy of the used ^{3}H-TDR [24-27,30-32]. The fraction of $E_{3_{H\text{-}TDR}}$ expresses the increase in U% by ^{3}H-TDR in the treated sample than that in the control sample (UControl %) represents the effectiveness of the drug dose ($E_{Drug\ dose}$) to increase H_G of the treated sample than that of the control sample ($H_{G.control}$) as a result of the induced cell cycle arrest [24-27, 30-32]. i.e. $E_{Drug\ dose} = H_G - H_{G.control}$ =increase in U% $\times E_{3_{H\text{-}TDR}}$ =(U%-$U_{Control}$%) $\times E_{3_{H\text{-}TDR}} = Li_0(Si\text{-}1) \times E_{3_{H\text{-}TDR}}$ (Equation 5), where (Si) is the Stimulating index ($Si = \frac{Li}{Li_{Control}}$), where Li and $Li_{Control}$ are the labelled indices of the treated and control samples by ^{3}H -TDR incorporation respectively.

Preparation of Homogenate Brain

Comparing the mechanical behavior of tumour response of the treated groups by that of the control groups is assessed by determining the growth constants of those tumours of different volumes along the corresponding periods [33,34]. The tumour growth constant at a certain time expresses the rate of the difference between Mitosis and Apoptosis with respect to the total number of the tumour cells (M - A) that characterize the tumour response at that time.

i.e. $(M - A) = \frac{\ln 2}{t_D}$, where in seconds [18-29].

The tumour histologic grade (H_G) that expresses tumour response can be identified from Equation 1 as follows:

$$H_G = \ln\left(\ln\frac{\ln 2}{t_D}\right)^2 \times C_0 \times h \times 23234.59 \text{ MeV} \quad \text{(Equation 6)},$$

where is number of the hypoxic cells in the tumour or number of the inoculated cells in the transplanted tumour in xenografted models [18-29]. Accordingly, alteration induced in tumour due to 4-HPR therapy expresses the effectiveness of the drug dose ($E_{Drug\ dose}$) to inhibit tumor growth. Thus, similar to the in-vitro model; energy yield by the drug dose can be identified from the in-vivo response as follows:

$E_{Drug\ dose} = (H_G - H_{G.control}) = \left[\ln\left(\ln\frac{\ln 2}{t_D}\right)^2_{Treated} - \ln\left(\ln\frac{\ln 2}{t_D}\right)^2_{Control}\right]$ 23234.59 MeV (Equation 7) [24-29].

Previously published data of *in-vitro* and *in-vivo* experiments were used for identifying and predicting the effectiveness of Fenretinide (4-HPR) alone and in combination with radiotherapy.

Fenretinide delays tumor growth *in vivo*

(1) Non-small cell lung cancer (NSCLC) cell line (A549) xenograft mouse model

As conducted and described by H. Xie., *et al.* [35]; Athymic nude mice [Cr: NIH (S), NIH Swiss nude, 6- to 9-week old] were divided into different groups (n = 10 of each group). The non-small cell lung cancer cell line (A549) lung cancer cells (4 × /0.1 ml) were injected subcutaneously into the right flank of each mouse. 4-HPR was freshly prepared once a week and protected from light and kept at 4°C as described previously [36,37]. Doses (10mg/ml or 40mg/ml) of 4-HPR or vehicle were administered by i.p. injection three times a week from day 8 to day 29 after injection of cells. Tumor volumes were measured twice a week.

(2) Lymphoma xenograft model

As conducted and described by Ajay K. Gopal., *et al.* [36]; Athymic mice (8 mice per group) were inoculated subcutaneously with 7 Ramos (Burkitt lymphoma) cells. Seventy-two hours after inoculation, mice were randomly assigned to treatment for 4 weeks with 4-HPR (250 μ g/d, 5 days per week) or solvent only for control group. Tumor volume was measured over time every four days from day 8 to day 30 after inoculation of cells.

(3) aRMS xenograft mouse model

As conducted and described by Martín, David Herrero., *et al.* [38]; Pediatric tumor alveolar rhabdomyosarcoma (aRMS) xenograft mouse model generated by subcutaneous injection of Rh4 cells engineered to constitutively express luciferase into immunocompromised NOD/Scidil2rg2/2 mice to analyze the effects of fenretinide *in vivo*. 3 ×10^6 Rh4-luc cells were re-suspended in PBS and injected s.c into the flanks of 6 weeks old NOD/Scid Il2rg2/2 (NSG) mice (Charles River, Sulzfeld, Germany). Mice bearing tumors were treated intraperitoneally after the tumor reached a volume of at least 100 with either sterile 0.9% NaCl or 4-HPR at a dose of 20 mg/kg daily for two weeks. Tumor growth was measured every day and mice were euthanized when reaching a tumor volume of 1500m^3 .

Fenretinide inhibits Ramos AW cell line proliferation *in vitro*

As conducted and described by Shan D, Gopal AK, Press OW [39]; Ramos AW cell line was maintained in log phase growth in RPMI 1640 supplemented with 12% fetal bovine serum, 2 mM glutamine, 1 mM sodium pyruvate, 100 units/ml penicillin, and 100 μ g/mL streptomycin. The effects of retinoids on malignant B-cell growth *in vitro* were determined by assessing [^{3}H] thymidine incorporation in Ramos cells [40].

Briefly, 10^4 cells were resuspended in 200 μ L culture medium and plated in 96-well, flat-bottomed microtiter plates. After incubating cells at 37°C for 48 h with 0, 0.1, 1, or 10 μ M of 4-HPR at 37°C for 48 h, 1 μ Ci of [^{3}H] thymidine/well was added, and cells were cultured for an additional 6 h. Cells incubated in medium without retinoids (0 μ M) were used as control. Cells were then harvested onto glass fiber filters with an automated harvesting system from Skatron, Inc. (Sterling, VA), and [^{3}H] thymidine uptake was assayed with a 4000-series liquid scintillation counter (Downers Grove, IL).

4-HPR in combination with irradiation in NSCLC cell line (A549) xenograft mouse model

As conducted and described by ZHU., *et al.* [4] Solitary tumors in Female nu/nu mice (4-6 weeks old) were produced by inoculation of NSCLC cell line A549 cells into the muscle of the right hind legs of the mice. When the tumors had grown to 7 - 8 mm in average diameter, the mice were randomly divided into 4 groups of 6 mice each. Groups of tumor-bearing mice were treated as: 1) intravenous injection of 4-HPR at a dose of 30 mg/kg, 2) local tumor irradiation alone, 3) 4-HPR (30 mg/kg, i.v.) 24h before local tumor irradiation and 4) Untreated mice served as controls. Before irradiation, mice were immobilized in a special jig, and tumors were centered in a 3-cm-diameter circular field. A single 10-Gy dose of gamma radiation was locally delivered using a dual-source $^{137}C_S$ unit at a dose rate of 6.25 Gy/min. The effect of each treatment on tumor response was assessed by tumor growth delay. Three orthogonal tumor diameters were measured using calipers at 1-day intervals until the tumors grew to at least 14 mm in mean diameter.

Results and Analysis

Identifying effectiveness of fenretinide

(1) Dose effect of 4-HPR on the murine NSCLC cell line (A549) tumor Model:

Doses of 10 and 40 mg/kg/d 4-HPR (molar mass = 391.55 g/mole) three times a week from day 8 to day 29 after injection of cells (9 doses) in human (70kg, 2.5L plasma) are equivalent to $\frac{(10 \text{ or } 40)\times 9\times 70\times 1000}{2.5\times 391.55}$ = 6435.959648 and 25743.83859 μM respectively. The results showed that treatment of mice with either dose of 4-HPR significantly suppressed A549 tumor growth relative to the vehicle-treated group. 4-HPR significantly suppresses lung cancer cell growth such that tumors in mice receiving the treatment of 6435.959648 M 4-HPR had a growth curve with t_D of 7 days [from 25 mm^3 at day 8 to 200 mm^3 at day 29 ($p < 0.001$)], those treated by 25743.83859 μ M 4-HPR had a growth curve with t_D of 10.27 days [from 25 mm^3 at day 8 to 103.2 mm^3 at day 29 ($p < 0.001$)]. While control group of tumors had a growth curve with t_D of 5.25 days [from 25 mm^3 at day 8 to 400.2 mm^3 at day 29 ($p<0.001$)] [35]. Thus, from Equation 7, energies yield by 6435.959648 and 25743.83859 μ M 4HPR in tumor xenograft of transplanted 4 ×10^6 A549 lung cancer cells were equivalent to:

$$E_{4HPR(6435.959648\,\mu M)} = \left[\ln\left(\ln\frac{\ln 2}{7\times 24\times 60\times 60}\right)^2 - \ln\left(\ln\frac{\ln 2}{5.25\times 24\times 60\times 60}\right)^2\right]$$

×4 ×10^6 cells ×23234.59 =3.95341197 ×10^9 MeV, while

$$E_{4HPR(25743.83859\,\mu M)} = \left[\ln\left(\ln\frac{\ln 2}{10.27\times 24\times 60\times 60}\right)^2 - \ln\left(\ln\frac{\ln 2}{5.25\times 24\times 60\times 60}\right)^2\right]$$

×4 ×10^6 cells ×23234.59 =9.0869642 ×10^9 MeV.

(2) Dose effect of 4-HPR on the murine lymphoma tumor model:

Dose of 250 μ g/20g/d 4-HPR (12.5mg/kg) (5 days per week for 4 weeks (total of 20 doses) (molar mass = 391.55 g/mole) in human (70kg, 2.5L plasma) is equivalent to $\frac{12.50\times 20\times 70\times 1000}{2.5\times 391.55}$ = 17877.66569 μ M. Monitoring tumor volume demonstrates that 4HPR delay the growth of lymphoma xenografts compared to the control. Tumors in mice receiving the treatment of 17877.66569 μ M 4-HPR had a growth curve with $t_Đ$ of 4.88 days [from 187 mm^3 at day 8 to 4250 mm^3 at day 30 ($p < 0.001$)]. On the other hand, the control group of tumors had a growth curve with $t_Đ$ of 3.6326 days [from 500 mm^3 at day 8 to 8750 mm^3 at day 23 (p <

0.001)] [36]. Thus, from Equation 7, energy yield by 17877.66569 μ M 4-HPR in tumor xenograft of transplanted 7 ×10^6 Ramos Burkitt lymphoma cells was equivalent to:

$$E_{4HPR(17877.66569\ \mu M)} = \left[\ln\left(\ln\frac{\ln 2}{4.88\times24\times60\times60}\right)^2 - \ln\left(\ln\frac{\ln 2}{3.6326\times24\times60\times60}\right)^2\right]$$

×7 ×10^6 cells ×23234.59=7.30038663 MeV.

Table 1 shows the identified energies yield by 4-HPR doses results from the above shown analysis to dose effect of 4-HPR doses on different murine tumor models ($p < 0.001$).

4-HPR dose in μ M	Energy yield by 4-HPR doses (E_{4HPR}) in MeV
6435.959648	3.95341197×10^9
17877.66569	7.30038663×10^9
25743.83859	9.0869642×10^9

Table 1: Shows the identified energies yield by 4-HPR doses in different murine tumor models ($p < 0.001$).

From Table 1, values of E_{4HPR} were perfectly power correlated ($r = 1$) with their corresponding doses of 4-HPR. Such perfect correlation boosts the confidence to establish the following efficient dose-energy model shown in Figure 1 and expressed in Equation 8 with a perfect fit ($R^2 = 1$) describes the energy yield by 4-HPR dose.

$E_{4HPR\ dose} = 2.04395305\times10^7\times(Dose_{\mu M})^{0.6003500401}$MeV (Equation 8), Where Dose is the 4HPRdose in μ M, $E_{4HPR\ dose}$ is the corresponding energy yield of that dose in MeV.

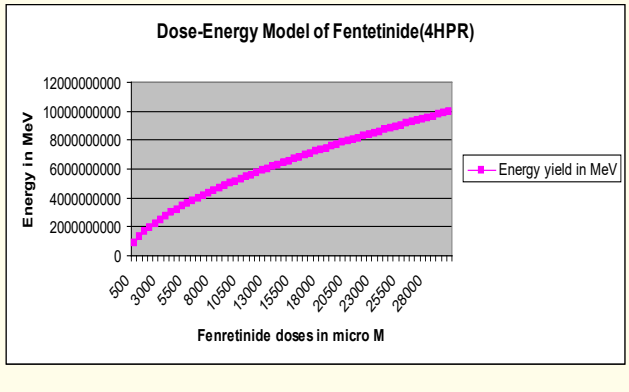

Figure 1: Shows energy in MeV yield by 4-HPR doses in μ M with perfect fit ($R^2=1$).

Predicting the effectiveness of 4-HPR *in-vivo* and *in-vitro*

(1) Predicting the effectiveness of 4-HPR in treating aRMS xenograft mouse model

The therapeutic response of aRMS tumor model can be predicted by knowing characteristics of the control tumor model and effectiveness of 4-HPR doses expressed by dose-energy model shown in Equation 8 as follows:

Tumor t_D of the control group of aRMS tumor model was 3.07 days [from 100 mm^3 at day 1 to 1500 mm^3 at day 12 after starting therapy ($p < 0.001$)] [38]. Doses of 20 mg/kg 4-HPR daily for two weeks (molar mass = 391.55 g/mole) (14 doses) in human (70 kg, 2.5L plasma) are equivalent to $\frac{20\times14\times70\times1000}{2.5\times391.55}$ = 20022.98557 μ M. From Equation 8, the energy yield by 20022.98557 μ M 4-HPR is 7.81436916 MeV. Accordingly, difference in tumor energy induced in treated group of aRMS tumor model of injected 3 ×10^6 Rh4-luc cells by 20022.98557 μ M 4-HP would be as follows:

$$\left[\ln\left(\ln\frac{\ln2}{t_{D.Treated}\times24\times60\times60}\right)^2 - \ln\left(\ln\frac{\ln2}{3.07\times24\times60\times60}\right)^2\right] \times 3\times10^6 \text{ cells} \times 23234.59 =$$

7.81436916 ×10^9MeV

Thus, the predicted tumor t_D of the treated group of aRMS tumor model prior therapy ($t_{D.Treated}$) would be equal to:

$$t_{D.Treated} = \frac{\ln 2\times e^{\sqrt{\frac{7.81436916\times10^9}{23234.59\times3\times10^6} + \ln\left(\ln\frac{\ln2}{3.07\times24\times60\times60}\right)^2}}}{24\times60\times60}$$

=6.45 days.

On the other hand, during treatment with 4-HPR at a dose of 20 mg/kg daily for two weeks significantly slowed down tumor growth compared to control mice. The actual tumor t_D of the treated group of aRMS tumor model after therapy was 100% identical to the predicted one [from 100 mm^3 at day 1 to 860 mm^3 at day 21 after starting therapy ($p < 0.001$)] [38] to strengthen the confidence in predicting the therapeutic *in-vivo* response to 4-HPR using characteristics of the control tumor and dose-energy model shown in Equation 8.

(2) Predicting the effectiveness of each of 4-HPR and irradiation alone or in combination in NSCLC (A549) model

1st Effectiveness of 4-HPR alone

Similarly, the therapeutic response of A549 tumor model to 4-HPR can be predicted as follows:

The range of the tumor of the control group of A549 tumor model was (18.72543319 → 22.79617954) days while its mean was 20.76080637 days [Mean diameter grew from 7.5 to 12.5

in 15.3 1.5 day (0.01 < p < 0.05)] [4]. A single dose of 30 mg/kg 4-HPR (molar mass = 391.55 g/mole) (1 dose) in human (70kg, 2.5L plasma) is equivalent to $\frac{30\times1\times70\times1000}{2.5\times391.55}$ = 2145.319883 μ M. From Equation 8, the energy yield by 2145.319883 μ M 4-HPR is 2.04424200 $\times10^9$ MeV. Accordingly, the range of the difference in tumor energy induced in treated group of A549 tumor model of injected 5 $\times10^6$ NSCLC cells by 2145.319883 μ M 4-HPR would be predicted equivalent to

$$\left[\ln\left(\ln\frac{\ln2}{t_{D.Treated}\times24\times60\times60}\right)^2-\ln\left(\ln\frac{\ln2}{18.72543319\rightarrow22.79617954\times24\times60\times60}\right)^2\right]\times5\times10^6 \text{ cells } 23234.59 = 2.04424200\times10^9 \text{ MeV}$$

While it's mean would be predicted equivalent to

$$\left[\ln\left(\ln\frac{\ln2}{t_{D.Treated}\times24\times60\times60}\right)^2-\ln\left(\ln\frac{\ln2}{20.76080637\times24\times60\times60}\right)^2\right]\times5\times10^6 \text{ cells } 23234.59 = 2.04424200\times10^9 \text{ MeV}$$

Thus, the interval of the predicted tumor of the treated group of A549 tumor model prior therapy ($t_{D.Treated}$) would be

$$\frac{\ln2\times e^{\sqrt{\frac{2.04424200\times10^9}{23234.59\times5\times10^6}+\ln\left(\ln\frac{\ln2}{18.72543319\rightarrow22.79617954\times24\times60\times60}\right)^2}}}{24\times60\times60} = 21.31608857 \rightarrow 25.99517022 \text{ days.}$$

While its mean would be $\frac{\ln2\times e^{\sqrt{\frac{2.04424200\times10^9}{23234.59\times5\times10^6}+\ln\left(\ln\frac{\ln2}{20.76080637\times24\times60\times60}\right)^2}}}{24\times60\times60}$ =23.6546143 days. Accordingly, the predicted time for the mean tumor diameter to grow from 7.5 to 12.5 would be (15.7 $\rightarrow$ 19.16) 17.4 1.7 days. On the other hand, the observation sample of the actual time for the mean tumor diameter of the treated group by 30 mg/kg 4-HPR to grow from 7.5 to 12.5 was 15.8 $\rightarrow$ 3.2 (12.6 19) days (0.01 < p < 0.05) [4]. The difference between these sample means was tested at the 0.05 level of significance (= 0.05) to determine whether significant or not. As α =0.05, then $t_{\alpha/2} = t_{0.025}$ =2.228 for degrees of freedom (d.f.) = 6+6-2=10 [41]. Rejecting the null hypothesis (H_0: difference between the sample means is not significant) if the t statistic (t): t $\leq$-2.228 or t $\geq$ 2.228. The pooled standard deviation (S_p= $\sqrt{\frac{(6-1)\times1.7^2+(6-1)\times3.2^2}{6+6-2}}$) was $\approx$ 2.562, whereas t ($\frac{17.4-15.8}{2.562\times\sqrt{\frac{1}{6}+\frac{1}{6}}}$) was $\approx$ 1.08. Since, -2.228 < t (1.08) < 2.228, therefore H_0 cannot be rejected, in other words the difference between the means of the predicted and the actual samples was not statistically significant. Moreover, the p-value corresponding to t = 1.08 (and the two-sided alternative hypothesis (H_1: difference between the means is significant) is 0.2 [41]. Since 0.2 exceeds 0.05(α), it reconfirms that H_0 (difference between the means is not significant) cannot be rejected. In addition, by knowing number/group (n = 6), standard deviation (s = 1.7), d.f. = n-1 = 5) and the t statistic for (1 -α = 0.99) (= 4.032 [36]), the 99% confidence interval for the predicted time would be 17.4 4.032 $\times\frac{1.7}{\sqrt{6}}$ (14.6 5.8 $\rightarrow$ 20.2) days [41]. Since the 99% confidence interval for the predicted time contained the whole observation sample of the actual time [(14.6 20.2) $\supset$ (12.6 $\rightarrow$ 19)] then the predicted interval was the 100% interval for the actual interval induced by 30 mg/kg 4-HPR [41].

2nd Effectiveness of radiotherapy alone

Similarly, the therapeutic response of A549 tumor model to a single 10-Gy irradiation dose (XRT) can be predicted as follows: The energy yield by the exposure to XRT of 10 Gy in tumor xenograft of transplanted 5×106 A549 cells of 7.5 (~ 0.1 g [41])is equivalent to $\frac{10 \text{ Joule}}{\text{kg}}\times\frac{6.242\times10^{12} \text{ MeV}}{\text{Joule}}\frac{\text{kg}}{1000 \text{ g}}\times0.1 \text{ g} = 6.242\times10^9$ MeV.

Accordingly, the interval of the difference in tumor energy induced in treated group of A549 tumor model of injected 5 $\times10^6$ NSCLC cells by XRT of 10 Gy would be predicted equivalent to

$$\left[\ln\left(\ln\frac{\ln2}{t_{D.Treated}\times24\times60\times60}\right)^2-\ln\left(\ln\frac{\ln2}{18.72543319\rightarrow22.79617954\times24\times60\times60}\right)^2\right]\times5\times10^6 \text{ cells } 23234.59 = 6.242\times10^9 \text{ MeV}$$

While it's mean would be predicted equivalent to

$$\left[\ln\left(\ln\frac{\ln2}{t_{D.Treated}\times24\times60\times60}\right)^2-\ln\left(\ln\frac{\ln2}{20.76080637\times24\times60\times60}\right)^2\right]\times5\times10^6 \text{ cells } 23234.59 = 6.242\times10^9 \text{ MeV}$$

Thus, the interval of the predicted tumor t_D of the treated group of A549 tumor model prior therapy ($t_{D.Treated}$) would be

$$\frac{\ln2\times e^{\sqrt{\frac{6.242\times10^9}{23234.59\times5\times10^6}+\ln\left(\ln\frac{\ln2}{18.72543319\rightarrow22.79617954\times24\times60\times60}\right)^2}}}{24\times60\times60} = 27.9145696$$

34.16546461 days.

While its mean would be $\frac{\ln2\times e^{\sqrt{\frac{6.242\times10^9}{23234.59\times5\times10^6}+\ln\left(\ln\frac{\ln2}{20.76080637\times24\times60\times60}\right)^2}}}{24\times60\times60}$ =31.03583877 days. Accordingly, the predicted time for the mean tumor diameter to grow from 7.5 to 12.5 would be (20.6 $\rightarrow$

25.2) 22.9 ± 2.3 days. On the other hand, the observation sample of the actual time for the mean tumor diameter of the treated group of A549 tumor model by XRT of 10 Gy to grow from 7.5 to 12.5 was 22.8 ± 3.7 (19.1 → 26.5) days (0.01 < p < 0.05)] [4]. Thus, the means of these samples (22.9, 22.8 days) were 99.7% identical to strengthens the confidence in predicting the tumor response to radiation prior XRT as well. Moreover, the 99% confidence interval for the predicted time would be 22.9 ± $4.032 \times \frac{2.3}{\sqrt{6}}$ (19.1 → 26.7) days [41] including the whole observation sample of the actual time [((19.1 → 26.7) ⊃ (19.1 → 26.5)] to confirm also that the predicted interval was the 100% interval for the actual interval induced by XRT of 10 Gy [41].

3rd Antitumor activity of combined therapy in A549 xenografts

Similarly, the therapeutic response of A549 tumor model to the combination of 4-HPR and XRT can be predicted as follows: The energy yield by 30 mg/kg 4-HPR and the exposure to XRT of 10 Gy as previously calculated was $2.04424200 \times 10^9 + 6.242 \times 10^9 = 8.286242 \times 10^9$ MeV

Accordingly, from Equation 7 the interval of the difference in tumor energy induced in treated group of A549 tumor model of injected 5 NSCLC cells by30 mg/kg 4-HPR and XRT of 10 Gy would be predicted equivalent to

$$\left[\ln\left(\ln\frac{\ln 2}{t_{D.Treated}\times 24\times 60\times 60}\right)^2 - \ln\left(\ln\frac{\ln 2}{18.72543319 \rightarrow 22.79617954\times 24\times 60\times 60}\right)^2\right]$$

$\times 5 \times 10^6$ cells$\times$ 23234.59 = 8.286242×10^9 MeV

While it's mean would be predicted equivalent to

$$\left[\ln\left(\ln\frac{\ln 2}{t_{D.Treated}\times 24\times 60\times 60}\right)^2 - \ln\left(\ln\frac{\ln 2}{20.76080637\times 24\times 60\times 60}\right)^2\right]$$

$\times 5 \times 10^6$ cells $\times$23234.59 = 8.286242×10^9 MeV

Thus, the interval of the predicted tumor t_D of the treated group of A549 tumor model prior therapy ($t_{D.Treated}$) would be

$$\frac{\ln 2\times e\sqrt{e^{\frac{8.286242\times 10^9}{23234.59\times 5\times 10^6}+\ln\left(\ln\frac{\ln 2}{18.72543319\rightarrow 22.79617954\times 24\times 60\times 60}\right)^2}}}{24\times 60\times 60} = 31.88885473$$

39.09946614 days.

While its mean would be $\frac{\ln 2\times e\sqrt{e^{\frac{8.286242\times 10^9}{23234.59\times 5\times 10^6}+\ln\left(\ln\frac{\ln 2}{20.76080637\times 24\times 60\times 60}\right)^2}}}{24\times 60\times 60}$ = 35.48773377 days. Accordingly, the predicted time for the mean tumor diameter to grow from 7.5 mm to 12.5mm by combining XRT of 10 Gy and 30 mg/kg 4-HPR would be (23.5 → 28.1) 26.15 ± 2.65 days. On the other hand, the observation sample of the actual time for the mean tumor diameter of the treated group of A549 tumor model by combining XRT of 10 Gy and 30 mg/kg 4-HPR to grow from 7.5 mm to 12.5 mm was 25.5 ± 4.9(20.6 → 30.4)days (0.01 < p < 0.05)] [41]. The difference between these sample means was tested at the 0.05 level of significance (α = 0.05) to determine whether significant or not. As α = 0.05, then $t_{\alpha/2} = t_{0.025} = 2.228$ for degrees of freedom (d.f.) = 6 + 6 - 2= 10 [42]. Thus, rejecting the null hypothesis (H_0: difference between these sample means is not significant) if the t statistic (t): t ≤ -2.228 or t ≥ 2.228. The pooled standard deviation ($S_P = \sqrt{\frac{(6-1)\times 2.65^2+(6-1)\times 4.9^2}{6+6-2}}$) was ≈3.939, whereas t ($\frac{26.15-25.5}{3.939\times\sqrt{\frac{1}{6}+\frac{1}{6}}}$) was ≈0.2858. Since, -2.228 < t (0.2858) < 2.228, therefore H_0 cannot be rejected, in other words the difference between the means of the predicted and the actual samples was not statistically significant. Moreover, the p-value corresponding to t = 0.2858 (and the two-sided alternative hypothesis (: difference between these sample means is significant) is 0.2 [42]. Since 0.2 exceeds 0.05(α), it reconfirms that (difference between these sample means is not significant) cannot be rejected. In addition, the means of these samples (26.15, 25.5) were 97.5% identical to strengthens the confidence in predicting the tumor response to the XRT combined with 4-HPR. Moreover, the 99% confidence interval for the predicted time would be 26.15 ± $4.032 \times \frac{2.65}{\sqrt{6}}$ (21.88 → 30.51) days [42] including the whole observation sample of the actual time [((21.88 → 30.51) ⊃ (20.6 → 30.4)] to confirm also that the predicted interval was the 100% interval for the actual interval induced by combining XRT of 10 Gy with 30 mg/kg 4-HPR[42].

(3) Predicting the effectiveness of 4-HPR to inhibit proliferation of Ramos AW cell line *in-vitro*

The in vitro effect of 0.1, 1 and 10 μ M fenretinide on the growth of Ramos cells was monitored by the [^{3}H] thymidine incorporation in cell DNA. Table 2 shows growth of the treated samples by 4-HPR as percentage of the control sample expressed by the Stimulating index ($Si = \frac{Li}{Li_{Control}}$) by -TDR incorporation. Data are representative of two concordant experiments [39].

4-HPR dose in μ M	%Si by ^{3}H -TDR incorporation
0 (control sample)	100%
0.1	105%
1	80%
10	20%

Table 2: shows %Si by ^{3}H-TDR incorporation in treated samples by 4-HPR with respect to control (p < 0.001).

The *in vitro* effects of fenretinide doses on the growth of the treated samples of Ramos cells can be predicted by knowing characteristics of the control sample and effectiveness of 4-HPR doses expressed by dose-energy model shown in Equation 8. For instance, the *in vitro* effect of 1 and 10 μ M fenretinide can be predicted by monitoring the *in vitro* effect of 0.1 μ M fenretinide on the growth of Ramos cells as follows: From Table 2, the Stimulating index (Si) of ^{3}H-TDR incorporation in treated samples of Ramos cells was increased by 5% at 0.1 μ M of 4-HPR dose relative to that of the control samples ($Si_{Control}$= 1).

From Equation 8, the energies yield by0.1, 1 and 10 μ M 4HPR are 5.13004147 ×10^6 , 2.04395305 ×10^7 and 8.14368480 ×10^7MeV respectively.

Accordingly, from Equation 5,

$$\frac{E_{4\text{-HPR }1\mu M}}{E_{4\text{-HPR }0.1\mu M}} = \frac{2.04395305\times10^7}{5.13004147\times10^6} = \frac{(1 - Si_{1M})}{0.05}$$, while

$$\frac{E_{4\text{-HPR }10\mu M}}{E_{4\text{-HPR }0.1\mu M}} = \frac{8.14368480\times10^7}{5.13004147\times10^6} = \frac{(1 - Si_{10M})}{0.05}.$$

Thus, the predicted values of $Si_{1\mu M}$ and $Si_{10\mu M}$ would be 20 and 80% which are 100% identical to the actual values have been identified by Shan D., *et al.* [39] and shown in Table 2 to clarify the consistency between the *in-vivo* and the *in-vitro* studies and predictability of outcomes of either assay from the other.

Discussion

The purpose of this study is optimizing 4-HPR therapy alone or in combination with radiotherapy by identifying the personalized dose that requires predicting the patient response before therapy. Analysis to results demonstrates the potent pro-apoptotic activity of 4-HPR in several cancer models and the matching between its predictable effectiveness *in-vivo* and *in-vitro*. This study used *in-vivo* tumor model in athymic mice which is commonly used to study tumorigenesis and *in-vitro* assay to identify efficacy of novel chemotherapeutics [43]. The *in-vivo* and *in-vitro* models for predicting responses to 4-HPR therapy alone or in combination with radiotherapy were similar to those presented for staging tumors clinically and pathologically in earlier studies [16-23]. The energy yield by 4-HPR doses in dose-energy model shown in Equation 8 was identified through *in-vivo* studies which confirmed and predicted through the presented *in-vitro* application as conducted and described in earlier studies [24-32]. Such matching strengthens the confidence in both assays so that results of either assay can be predicted from results of the other one as shown in section of results and analysis. Thus, the personalized dose can be identified by predicting the patient response prior to therapy which can be checked through either assay. Thus, a possible decrease in risks of chemo-resistant or treatment failure in 4-HPR therapy might be avoided. The patient response to 4-HPR alone or in combination with XRT can be predicted by identifying each of the patient's histologic grade ($H_{G.Control}$)- *in-vitro* through ^{3}H-proliferation assay [16,21,22,24-26 and 30-32] or *in-vivo* through medical imaging [18-29] -and the energy yield by the administered dose as shown in section of results and analysis. In addition, predicting the outcomes of experiments of either assay from the other contributes to decrease the number of sacrificed animals in the *in-vivo* studies as well as the replication of samples in the *in-vitro* studies. Accordingly, applying such protocol in research also would reduce costs and time significantly and consequently enhance the production of cheap drugs.

Such technique is valid for predicting the therapeutic responses to all non-cell-cycle specific antitumor drugs as 4-HPR [24-27]. With respect to cell-cycle specific antitumor drugs as docetaxel and AT9283, scheduling regimens should be taken in consideration to construct their dose-energy models [28,29].

Dose-energy model shown in Equation 8 was possible to be identified in opposite way from the *in-vitro* assay using ^{3}H-Thymidine incorporation in samples of cell line treated with different doses of 4-HPR and then the therapeutic *in-vivo* responses in different models of xenografted tumors in mice can be predicted without a need to sacrifice great number of animals to be identified as shown in predicting effectiveness of 4-HPR alone in treating aRMS and NSCLC models or in combination with XRT in NSCLC model. Predicting the therapeutic response to 4-HPR *in-vivo* and the *in-vitro* with an almost perfect accuracy provides a clear-cut criterion for accepting that the effect on the histologic grade induced by adding 4-HPR is equivalent to the energy yield by the drug dose, and strengthens the confidence in $E_{4HPR\ dose}$ identified *in-vivo* using murine tumor models or that derived from the presented estimation model shown in Equation 8 as well.

The efficient dose-energy model (R^2= 1) of 4-HPR enables to find out dose equivalency between 4-HPR doses and other drugs used for therapeutic interventions. The use of 4-HPR in the established cancer therapies is limited by its general toxicity. Thus, targeting the development of new treatment modalities, several

studies recommended other anti-cancer agents to be used in combination with 4-HPR allowing the use of a much lower dose of either and thus decrease the drug side effects. In this respect, the differentiations between treatments with 4-HPR only or in combination with other chemotherapeutic agent or radiotherapy should be assessed by identifying the effect (energy yield) of the combined dose *in-vivo* or *in-vitro* as shown in section of results and analysis.

Thereafter, the corresponding dose of 4-HPR only that yields the equivalent energy to that of the combined dose can be derived from the established dose-energy model of current approach shown in Equation 8 and compared to that yield by the combined dose. If there will be a significant dose reduction by the combined dose that would result in a minimal toxicity accompanied by the same inhibition to tumor growth compared to that induced by 4-HPR only, then applying the combined dose becomes obligatory. This strategy will hopefully be translated into optimal therapies for human cancers to emphasize the importance of the individual patient treatment planning to provide a protection against possible treatment failure.

Conclusion

Effectiveness of 4-HPR *in-vivo* and *in-vitro* is identical and predictable regardless to stage or type of the disease. Dose-energy model enables to evaluate and differentiate between administering 4-HPR alone or in combination with radiotherapy. Targeting patient-personalized effective dose, patient-specific histologic grade ($H_{G.Control}$) and dose-energy model of 4-HPR are reliable to predict the patient's response prior to therapy.

Conflict of Interest

The author declares that there is no conflict of interest concerning this paper.

Supplementary File

Brief Commentary

Background: Although the ability of Fenretinide (4-HPR) to inhibit growth of cancer and metastasis has been confirmed *in-vitro* and *in-vivo*, no relationship has been determined between such ability in each assay. Also, the antitumor targets of applying 4-HPR alone or in combination with radiotherapy have not yet been identified to for optimizing therapy.

Translational Significance: Dose-energy model to estimate the energy yield by 4-HPR dose was constructed to predict patient response prior to therapy. The predicted responses to 4-HPR in the presented cancer models were 100% identical to those exhibited actually *in-vitro* or *in-vivo* (alone and in combination with radiotherapy).

Clinical Practise points

- Fenretinide (4-HPR) is a synthetic retinoid that has been tested in clinical trials as a cancer therapeutic and chemo preventive agent.
- Although the ability of 4-HPR to inhibit growth of cancer and metastasis has been confirmed *in vitro* and *in vivo*, no relationship has been determined between such ability in each assay.
- Also, the antitumor target of 4-HPR has not yet been identified whether applied alone or in combination with radiotherapy to optimize therapy and provide a protection against treatment failure by predicting the response of patients before therapy.
- In the present study, we identify for the first time a predictable antitumor target of 4-HPR whether applied alone or in combination with radiotherapy and report that efficacy of 4-HPR is identical *in-vitro* and *in-vivo* regardless to the stage or type of the disease.

Microabstract

This research aims to identify and predict the effectiveness of Fenretinide (4-HPR) *in-vitro* and *in-vivo* alone or in combination with radiotherapy. Dose-energy model was constructed to estimate the energy yield by 4-HPR dose. Predicted responses to 4-HPR in cancer models were identical to those exhibited actually *in-vivo* (alone or in combination with radiotherapy) or *in-vitro* regardless to type of disease.

Highlights

<The ability of 4HPR to inhibit cancer growth has been confirmed *in-vitro* and *in-vivo*>

<Efficacy of 4HPR alone or in combination with radiotherapy hasn't yet been identified>

<Dose-energy model was assessed to identify energies yield by 4HPR doses *in-vivo*>

<Prediction of the response to 4HPR was identical to those exhibited *in-vivo* or *in-vitro*>

<Efficacy of 4HPR in both assays is identical regardless to stage or type of disease>

Bibliography

1. Huang ME., *et al.* "Use of all-trans retinoic acid in the treatment of acute promyelocytic leukemia". *Blood* 72.2 (1988): 567-572.

2. Tang XH and Gudas L J. "Retinoids, retinoic acid receptors, and cancer". *Annual Review of Pathology* 6 (2011): 345-364.

3. Bosch A., *et al.* "Reversal by RARα agonist AM580 of c-Myc-induced imbalance in RARα/RARγ expression during MMTV-Mmyc tumorigenesis". *Breast Cancer Research* 14.4 (2012): R121.

4. Zhu G., *et al.* "Polymeric retinoid prodrug PG-4HPR enhances the radiation response of lung cancer". *Oncology Reports* 18.3 (2007): 645-651.

5. Benelli R., *et al.* "The chemopreventive retinoid 4HPR impairs prostate cancer cell migration and invasion by interfering with FAK/AKT/GSK3beta pathway and beta-catenin stability". *Molecular Cancer* 9 (2010): 142.

6. Decensi A., *et al.* "Pilot study of high dose fenretinide and vitamin A supplementation in bladder cancer". *European Journal of Cancer* 30A (1994): 1909-1910.

7. O'Donnell PH., *et al.* "N-(4-hydroxyphenyl) retinamide increases ceramide and is cytotoxic to acute lymphoblastic leukemia cell lines, but not to non-malignant lymphocytes". *Leukemia* 16.5 (2002): 902-910.

8. Asumendi A., *et al.* "Implication of mitochondria-derived ROS and cardiolipin peroxidation in N-(4- hydroxyphenyl) retinamide-induced apoptosis". *British Journal of Cancer* 86.12 (2002): 1951-1956.

9. Dolle P. "Developmental expression of retinoic acid receptors (RARs)". *Nuclear Receptor Signaling* 7 (2009): e006.

10. Sabichi AL., *et al.* "Phase III prevention trial of fenretinide in patients with resected non-muscle-invasive bladder cancer". *Clinical Cancer Research* 14.1 (2008): 224-229.

11. Decensi A., *et al.* "Randomized double-blind 2 × 2 trial of low-dose tamoxifen and fenretinide for breast cancer prevention in high-risk premenopausal women". *Journal of Clinical Oncology* 27.23 (2009): 3749-3756.

12. Delia D., *et al.* "N-(4-hydroxyphenyl) retinamide induces apoptosis of malignant hemopoietic cell lines including those unresponsive toretinoic acid". *Cancer Research* 53.24 (1993): 6036-6041.

13. Benbrook D., *et al.* "Differential retinoic acid radiosensitization of cervical carcinoma cell lines". *Clinical Cancer Research* 3.6 (1997): 939-945.

14. Scribner J., *et al.* "Retinoids enhance cisplatin-based chemoradiation in cervical cancer cells *in vitro*". *Gynecologic Oncology* 85.1 (2002): 223-225.

15. Zou C., *et al.* "Combined effect of chemopreventive agent n-(4-hydroxyphenyl) retinamide (4-hpr) and gamma-radiation on bladder cancer cell lines". *International Journal of Oncology* 13.5 (1998): 1037-1041.

16. Emad Y Moawad. "Pathologic Cancer Staging by Measuring Cell Growth Energy". *Cancer and Oncology Research* 1.3 (2013): 69 - 74.

17. Moawad Emad Y. "Mass-Energy Conversion in the Decaying System and Doubling Time-Energy Conversion in the Biological System". *Journal of Physics Research and Reviews* 1.1 (2015): 1-13.

18. Emad Moawad. "Isolated System Towards a Successful Radiotherapy Treatment, Nuclear Medicine and Molecular Imaging". 44.2 (2010):123-136

19. Emad Y Moawad. "Radiotherapy and risks of tumor regrowth or inducing second cancer". *Cancer Nanotechnology* 2 (2011): 81-93

20. Emad Y Moawad. "Safe Doses and Cancer Treatment Evaluation". *Cancer and Oncology Research* 1.1 (2013): 6 - 11.

21. Emad Y Moawad. "Clinical and Pathological Cancer Staging at the Nanoscale". *Cancer Nanotechnology* 3 (2012): 37-46.

22. Emad Y Moawad. "Reconciliation between the clinical and pathological staging of cancer". *Comparative Clinical Pathology* 23.2 (2014): 255-262.

23. Emad Y Moawad. "Safe Cancer Screening for Patients after Lumpectomy, Survivors, and Healthy Subjects". *Cancer and Oncology Research* 1.2 (2013): 15 - 23.

24. Moawad EY. "Administering the optimum dose of l-arginine in regional tumor therapy". *Indian Journal of Clinical Biochemistry* 29.4 (2014): 442-451.

25. Moawad EY. "Identifying the optimal dose of ritonavir in the treatment of malignancies". *Metabolic Brain Disease* 29.2 (2014): 533-540.

26. Moawad and Emad Y. "Identifying and Predicting the Effec-

tiveness of Carboplatin *In vivo* and *In vitro* and Evaluating its Combination with Paclitaxel". Indian Journal of Gynecologic Oncology 13.1 (2015): 1-9.

27. Moawad EY. "Predicting Effectiveness of Imatinib Mesylate in Tumors Expressing Platelet-Derived Growth Factors (PDGF-AA, PDGF-BB), Stem Cell Factor Ligands and Their Respective Receptors (PDGFR-α, PDGFR-β, and c-kit)". *Journal of Gastrointestinal Cancer* 46.3 (2015): 272-283.

28. Moawad EY. "Optimizing and predicting the *in vivo* activity of AT9283 as a monotherapy and in combination with paclitaxel". *Journal of Gastrointestinal Cancer* 46.4 (2015): 380-389.

29. Emad Y. Moawad. "Optimal standard regimen and predicting response to docetaxel therapy". *Mutation Research - Fundamental and Molecular Mechanisms of Mutagenesis* 770 (2014): 120-127.

30. Emad Y Moawad. "The Mechanism by which Chronic Myeloid Leukemia Responds to Interferon-α Treatment". *Advances in Pharmacology and Pharmacy* 1.2 (2013): 88-94.

31. Emad Y Moawad. "Induction of Rheumatoid Arthritis and Response to Tyrosine Kinase Inhibitors". *Universal Journal of Medical Science* 1.2 (2013): 50-55.

32. Moawad EY. "Induction of multiple sclerosis and response to tyrosine kinase inhibitors". *Indian Journal of Clinical Biochemistry* 29.4 (2014): 491-495.

33. Kyprianou., *et al.* "Programmed cell death during regression of the MCF-7 human breast cancer following estrogen ablation". *Cancer research* 51.1 (1991): 162-166.

34. Steel GG. "Growth Kinetics of Tumours. Cell Population Kinetics in Relation to the Growth and Treatment of Cancer". Oxford. United Kingdom: Clarendon Press, 1977.

35. Xie., *et al.* "Identification of mammalian target of rapamycin as a direct target of fenretinide both *in vitro* and *in vivo*". *Carcinogenesis* 33.9 (2012): 1814-1821.

36. Gopal AK., *et al.* "Fenretinide enhances rituximab-induced cytotoxicity against B-cell lymphoma xenografts through a caspase-dependent mechanism". *Blood* 103.9 (2004): 3516-3520.

37. Formelli F., *et al.* "Therapeutic effects of the combination of fenretinide and all-trans-retinoic acid and of the two retinoids with cisplatin in a human ovarian carcinoma xenograft and in a cisplatin-resistant sub-line". *European Journal of Cancer* 36.18 (2000): 2411-2419.

38. Martín., *et al.* "Cell-Based Small-Molecule Compound Screen Identifies Fenretinide as Potential Therapeutic for Translocation-Positive Rhabdomyosarcoma." *PloS one* 8.1 (2013): e55072.

39. Shan D., *et al.* "Synergistic effects of the fenretinide (4-HPR) and anti-CD20 monoclonal antibodies on apoptosis induction of malignant human B cells". *Clinical Cancer Research* 7.8 (2001): 2490-2495.

40. Funakoshi S., *et al.* "Inhibition of human B-cell lymphoma growth by CD40 stimulation". *Blood* 83.10 (1994): 2787-2794.

41. Freund., *et al.* "Modern elementary statistics". Englewood Cliffs, New Jersey: Prentice-Hall, 256 (1967).

42. Zhou., *et al.* "99mTc-labeled cyclic RGD peptides for noninvasive monitoring of tumor integrin avb3 expression". *Molecular Imaging* 10.5 (2011): 386-397.

43. Zhang L., *et al.* "The oncogene phosphatidylinositol 3V-kinase catalytic subunit a promotes angiogenesis via vascular endothelial growth factor in ovarian carcinoma". *Cancer Research* 63.14 (2003): 4225-4231.

Volume 1 Issue 3 September 2017